

# Nematic liquid crystalline polymer films for gas separation

**Citation for published version (APA):**

Kloos, J., Lub, J., Houben, M., Borneman, Z., Nijmeijer, K., & Schenning, A. P. H. J. (2023). Nematic liquid crystalline polymer films for gas separation. *Liquid Crystals*, 50(3), 414-422.  
<https://doi.org/10.1080/02678292.2022.2134597>

**DOI:**

[10.1080/02678292.2022.2134597](https://doi.org/10.1080/02678292.2022.2134597)

**Document status and date:**

Published: 01/01/2023

**Document Version:**

Publisher's PDF, also known as Version of Record (includes final page, issue and volume numbers)

**Please check the document version of this publication:**

- A submitted manuscript is the version of the article upon submission and before peer-review. There can be important differences between the submitted version and the official published version of record. People interested in the research are advised to contact the author for the final version of the publication, or visit the DOI to the publisher's website.
- The final author version and the galley proof are versions of the publication after peer review.
- The final published version features the final layout of the paper including the volume, issue and page numbers.

[Link to publication](#)

**General rights**

Copyright and moral rights for the publications made accessible in the public portal are retained by the authors and/or other copyright owners and it is a condition of accessing publications that users recognise and abide by the legal requirements associated with these rights.

- Users may download and print one copy of any publication from the public portal for the purpose of private study or research.
- You may not further distribute the material or use it for any profit-making activity or commercial gain
- You may freely distribute the URL identifying the publication in the public portal.

If the publication is distributed under the terms of Article 25fa of the Dutch Copyright Act, indicated by the "Taverne" license above, please follow below link for the End User Agreement:

[www.tue.nl/taverne](http://www.tue.nl/taverne)

**Take down policy**

If you believe that this document breaches copyright please contact us at:

[openaccess@tue.nl](mailto:openaccess@tue.nl)

providing details and we will investigate your claim.



## Nematic liquid crystalline polymer films for gas separation

Joey Kloos, Johan Lub, Menno Houben, Zandrie Borneman, Kitty Nijmeijer & Albert P. H. J. Schenning

To cite this article: Joey Kloos, Johan Lub, Menno Houben, Zandrie Borneman, Kitty Nijmeijer & Albert P. H. J. Schenning (2023) Nematic liquid crystalline polymer films for gas separation, *Liquid Crystals*, 50:3, 414-422, DOI: [10.1080/02678292.2022.2134597](https://doi.org/10.1080/02678292.2022.2134597)

To link to this article: <https://doi.org/10.1080/02678292.2022.2134597>



© 2022 The Author(s). Published by Informa UK Limited, trading as Taylor & Francis Group.



[View supplementary material](#)



Published online: 20 Oct 2022.



[Submit your article to this journal](#)



Article views: 766



[View related articles](#)







[View Crossmark data](#)



Citing articles: 1 [View citing articles](#)

## Nematic liquid crystalline polymer films for gas separation

Joey Kloos <sup>a</sup>, Johan Lub <sup>b</sup>, Menno Houben<sup>a</sup>, Zandrie Borneman<sup>a</sup>, Kitty Nijmeijer <sup>a</sup>  
and Albert P. H. J. Schenning <sup>b</sup>

<sup>a</sup>Membrane Materials and Processes, Department of Chemical Engineering and Chemistry, Eindhoven University of Technology, Eindhoven, The Netherlands; <sup>b</sup>Stimuli-responsive Functional Materials and Devices, Department of Chemical Engineering and Chemistry, Eindhoven University of Technology, Eindhoven, The Netherlands

### ABSTRACT

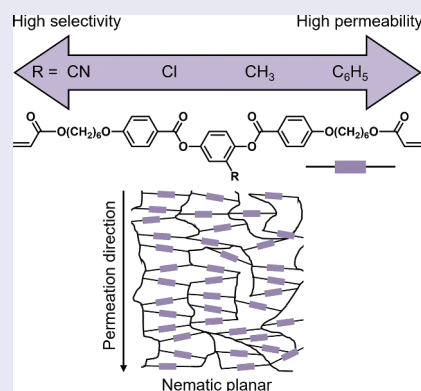
The gas separation performances of free-standing planar aligned nematic LC polymer films were investigated for gas separations of He, CO<sub>2</sub>, CH<sub>4</sub> and Xe. The films consist of derivatives of 1,4-phenylene bis(4-((6-(acryloyloxy)hexyl)oxy)benzoate)s with respective cyano, chloro, methyl and phenyl substituents on the central aromatic cores. Two new LC derivatives of 1,4-phenylene bis(4-((6-(acryloyloxy)hexyl)oxy)benzoate)s were successfully synthesised and fully characterised. Single gas permeation and sorption data show increasing gas permeabilities with increasing steric size of the substituents while the ideal gas selectivity of He over CH<sub>4</sub> and He over CO<sub>2</sub> decreases. The sorption coefficient of all films is independent of the LC substituents, while the subsequently extracted diffusion coefficient for the films with a phenyl substituent is three times higher compared to the films with a cyano substituent, demonstrating that the steric size of the LC substituents mainly affects the diffusion of gasses rather than the solubility of the gases. Irrespective of a methyl or a phenyl substituent, a larger kinetic diameter of Xe gives a 20 times lower diffusion coefficient compared to the smaller species (CO<sub>2</sub>).

### ARTICLE HISTORY

Received 15 August 2022  
Accepted 6 October 2022

### KEYWORDS

Nematic phase; steric size effect; gas separation; polymer films




## 1. Introduction

Thermotropic liquid crystal (LC) molecules are small molecules that can self-assemble into various nanostructures and provide excellent control over the molecular order and orientation of the molecules [1–5]. Nanostructures like nematic and smectic morphologies can be obtained, which differ in positional order of the LC monomers, by varying the temperature in the fabrication process (Figure 1(b)). Subsequent crosslinking of the LC monomers is necessary to obtain free-standing LC polymer films [2,3].

Safeguarding a sustainable future results in the necessity to lower our greenhouse gas emissions (CO<sub>2</sub> and CH<sub>4</sub>) and makes separations such as CO<sub>2</sub>/CH<sub>4</sub> and CO<sub>2</sub>/N<sub>2</sub> crucial and relevant [6–9]. Polymeric membrane processes are often used in gas separation processes due to their high energy efficiency, low operating costs and easy scalability compared to other separation technologies [10–13]. Using LC materials that can self-assemble into nanostructured polymer films provide control over the molecular order and alignment of the film-building blocks and can be used to tune the gas separation properties. However, the gas separation

**CONTACT** Albert P. H. J. Schenning  [a.p.h.j.schenning@tue.nl](mailto:a.p.h.j.schenning@tue.nl)

 Supplemental data for this article can be accessed online at <https://doi.org/10.1080/02678292.2022.2134597>.

© 2022 The Author(s). Published by Informa UK Limited, trading as Taylor & Francis Group. This is an Open Access article distributed under the terms of the Creative Commons Attribution License (<http://creativecommons.org/licenses/by/4.0/>), which permits unrestricted use, distribution, and reproduction in any medium, provided the original work is properly cited.

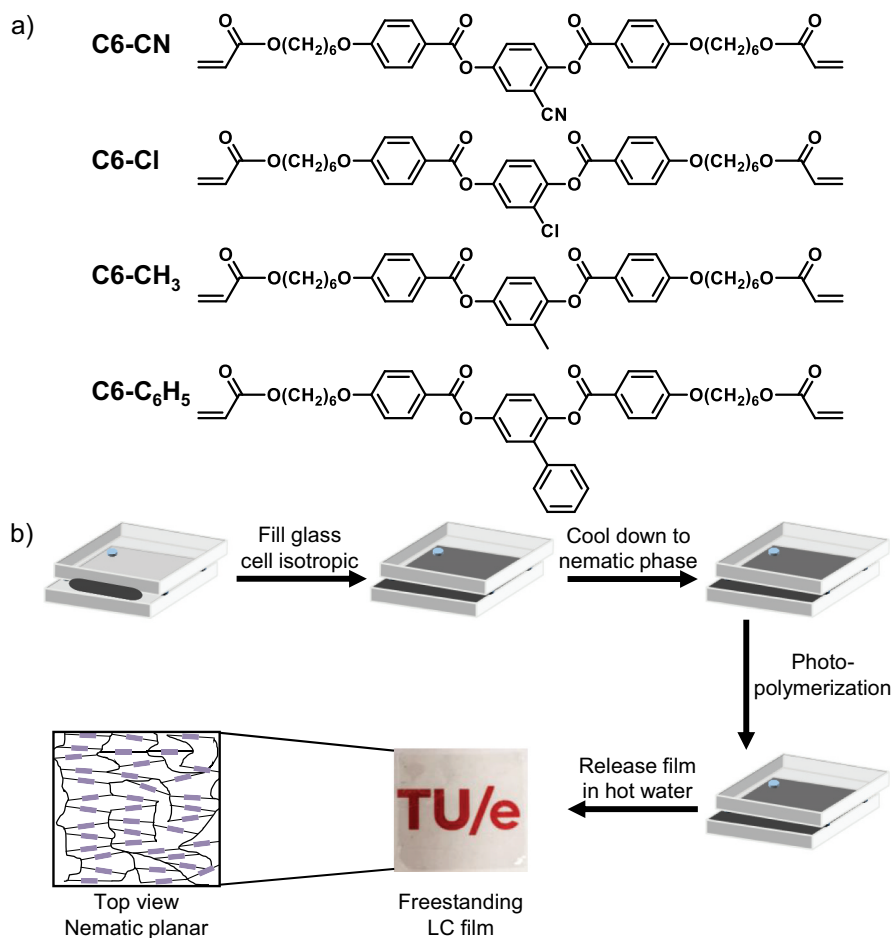


**Figure 1.** (Color online) (a) the molecular structures of the nematic LCs under investigation. (b) schematic representation of the fabrication process of nematic LC films. The purple rods represent the aromatic cores of the LCs.

performances of such nanostructured materials have hardly been reported in literature.

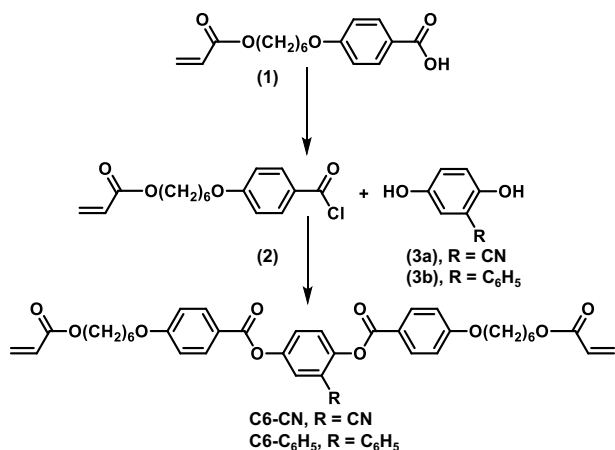
In our previous work, we investigated smectic LC polymer films for gas separation [14]. Now, we investigate the effect of several substituents on the gas separation properties of free-standing planar aligned nematic LC polymer films with respective cyano, chloro, methyl and phenyl substituents (C6-CN, C6-Cl, C6-CH<sub>3</sub> and C6-C<sub>6</sub>H<sub>5</sub> in Figure 1(a)) for gas separations of He, CO<sub>2</sub>, CH<sub>4</sub> and Xe. Several nematic LC films are fabricated and characterised consisting of LCs with different substituents, which differ in steric size, on the central aromatic cores of the di-acrylate monomers (Figure 1(a)). The gas separation properties of the prepared films are characterised by single gas sorption and permeation measurements to study the effect of the substituents on gas permeability and ideal gas selectivity. Moreover, the effect of the kinetic diameter of different gas species (CO<sub>2</sub> and Xe) on the gas separation properties of nematic LC films was studied by comparing single gas permeation and sorption data of nematic LC films with different substituents.

## 2. Materials and methods

### 2.1. Chemicals

2-chloro-1,4-phenylene bis(4-((6-(acryloyloxy)hexyl)oxy)benzoate) (C6-Cl) was prepared as described in our previous publication [15]. 2-methyl-1,4-phenylene bis(4-((6-(acryloyloxy)hexyl)oxy)benzoate) (C6-CH<sub>3</sub>) was obtained from Merck Life Science. The synthesis of 2-cyano-1,4-phenylene bis(4-((6-(acryloyloxy)hexyl)oxy)benzoate) (C6-CN) and [1,1'-biphenyl]-2,5-diyl bis(4-((6-(acryloyloxy)hexyl)oxy)benzoate) (C6-C<sub>6</sub>H<sub>5</sub>) is outlined in Scheme 1 (section 3.1). 4-(6-(acryloyloxyhexyloxy)benzoic acid (**1**) was obtained from Synthon and [1,1'-biphenyl]-2,5-diol (**3b**) from TCI. 2-cyanohydroquinone (**3a**) was made according to a literature procedure [16].

All other chemicals that were used for the synthesis of the LC monomers were obtained from Sigma-Aldrich. Irgacure 819 was supplied by Ciba. *t*-Butylhydroquinone was purchased from Merck Life Science. For permeation and sorption measurements, the gasses



**Scheme 1.** Synthetic routes to 2-cyano-1,4-phenylene bis(4-((6-(acryloyloxy)hexyl)oxy)benzoate) (**C6-CN**) and [1,1'-biphenyl]-2,5-diyl bis(4-((6-(acryloyloxy)hexyl)oxy)benzoate) (**C6-C<sub>6</sub>H<sub>5</sub>**).

He (5.0 grade), CO<sub>2</sub> (4.5 grade) and CH<sub>4</sub> (4.5 grade) were obtained from Linde Gas (the Netherlands). Xe (5.0 grade) was supplied by Westfalen BV (the Netherlands). All reagents were used as received without further purification.

## 2.2. Film preparation

LC mixtures with 0.5 wt% photoinitiator (Irgacure 819) and 0.1 wt% inhibitor (*t*-Butyl-hydroquinone) were prepared by dissolving the compounds in a minimum amount of dichloromethane and subsequently removing the solvent after mixing (see Figure 1 for the chemical structures of the LCs and fabrication process). Planar aligned nematic films were fabricated by processing the LC mixtures in the nematic phase by capillary suction between two 20 μm spaced glass plates. The glass plates were cleaned before use with isopropanol in an ultrasonic bath for 30 min, dried with N<sub>2</sub> and treated with UV ozone for 20 min. To obtain planar alignment, the glass plates were functionalised with a rubbed polyimide layer (Optimer AL 1254; JSR Corporation, Toyo Japan). Glass cells were prepared by gluing two glass plates together with glue that contained 20 μm glass spacer beads. The glass cells were filled with the LC mixture and placed inside a temperature-controlled N<sub>2</sub> box, in which the glass cells were cooled from the isotropic phase to the nematic phase using a cooling rate between 1°C/min and 2°C/min. The planar aligned LC monomers were polymerised by exposing the samples for 10 min to an unfiltered spectrum of a collimated EXFO Omnicure S2000 UV lamp with a light intensity of 20 mW/cm<sup>2</sup> in the range of 320–390 nm. Free-standing films were obtained by carefully opening the glass cells in water at 80°C.

## 2.3. Characterisation

Nuclear magnetic resonance (NMR) spectra were recorded on a 400 MHz Bruker Avance III HD spectrometer in deuterated chloroform with tetramethyl silane (TMS) used as internal standard.

Matrix-assisted laser desorption/ionisation time-of-flight mass spectrometry (MALDI-TOF MS) was performed on a Bruker Autoflex Speed MALDI-MS instrument using CHCA (α-cyano-4-hydroxycinnamic acid) as matrix.

Attenuated total reflection Fourier transform infrared spectroscopy (ATR FT-IR) spectra were recorded at room temperature on a Varian-Cary 3100 FT-IR spectrometer equipped with a golden gate attenuated total reflectance (ATR) sampling accessory. Scans were taken over a range of 4000 – 650 cm<sup>-1</sup> with a spectral resolution of 4 cm<sup>-1</sup> and 50 scans per spectrum.

Polarising optical microscopy (POM) was performed using a Leica DM 2700 M optical microscope equipped with two polarisers that were operated either crossed or parallel with the sample in between a Linkam hot-stage THMS600 with a Linkam TMS94 controller and a Leica DFC420 C camera.

Differential scanning calorimetry (DSC) measurements were recorded in hermetic *T*-zero aluminium sample pans using a TA Instruments Q2000 DSC equipped with a cooling accessory. The DSC measurements were performed with three cycles of heating and cooling at a rate of 2°C/min with an isothermal equilibration of 3 min after each heating or cooling ramp.

Medium- and wide-angle X-ray scattering (MAXS/WAXS) measurements were recorded on a GaneshaLab instrument equipped with a Genix-Cu ultralow divergence source producing X-ray photons of wavelength 1.54 Å and a flux of 108 photons per second. Diffraction patterns were collected on a Pilatus 300 K silicon pixel detector with 487 × 619 pixels of 172 μm<sup>2</sup>.

## 2.4. Single gas performances

Single gas permeation measurements of He, CO<sub>2</sub>, CH<sub>4</sub> and Xe were performed in a custom-built permeation setup and have been carried out according to a literature procedure [14]. The single gas permeabilities were determined from the steady-state pressure increase in time in a calibrated volume at the permeate side of the film at a temperature of 40°C and a feed pressure of 6 bar. The order of the measured gasses was kept constant for all films (He, CH<sub>4</sub>, Xe and CO<sub>2</sub>) because CO<sub>2</sub> could induce swelling of the films. The ideal gas selectivity (α<sub>*i*/*j*</sub>) was calculated from the single gas permeabilities by using Equation (1).

$$\alpha_{i/j} = \frac{P_i}{P_j} \quad (1)$$

In Equation (1)  $P_i$  is the permeability of gas species  $i$  (Barrer) and  $P_j$  is the permeability of gas species  $j$  (Barrer).

## 2.5. Gas sorption

The gas permeability through dense polymer membranes is well described by the solution diffusion model, which states that the gas permeability ( $P_i$ ) is defined as the product of the diffusion coefficient ( $D_i$ ) and the solubility coefficient ( $S_i$ ) of a certain gas species [17,18]. The diffusion coefficient and the solubility coefficient highly depend on a combination of parameters such as the kinetic diameter, critical temperature and molecular interactions via the quadrupole moments of the gas species. These parameters are shown in Table 1 [19].

Gas sorption of  $\text{CO}_2$  and Xe was measured at 6 bar and  $40^\circ\text{C}$  with a magnetic suspension balance, using a Rubotherm series IsoSORP® sorption instrument, to investigate the effect of the different substituents and the effect of the kinetic diameter of the measured gasses on the gas separation properties of nematic LC films. The measurements and the solubility coefficient of the gasses were determined as described in our previous publication [14]. The  $\text{CO}_2$  and Xe diffusion coefficients were calculated by filling in the obtained sorption and permeability data in Equation (2).

$$D_i = \frac{P_i}{S_i} \quad (2)$$

In Equation (2),  $D_i$  is the diffusion coefficient ( $\text{cm}^2/\text{s}$ ),  $P_i$  the permeability (Barrer) and  $S_i$  the solubility coefficient ( $\text{cm}^3 \text{STP}/(\text{cm}^3 \cdot \text{cmHg})$ ) of a certain gas species.

## 3. Results and discussion

### 3.1. Synthesis and characterisation of the liquid crystalline molecules and mixtures

The effect of several substituents on the gas separation properties of planar aligned nematic LC films was investigated by preparing LC monomers with respective cyano, chloro, methyl and phenyl substituents (**C6-CN**, **C6-Cl**, **C6-CH<sub>3</sub>** and **C6-C<sub>6</sub>H<sub>5</sub>** in Figure 1(a)). These substituents were selected for their difference in steric size (cyano < chloro < methyl < phenyl). However, it must be noted that the polar cyano and chloro groups in **C6-CN** and **C6-Cl** can lead to improved interactions with  $\text{CO}_2$ , which can lead to enhanced  $\text{CO}_2$  permeability and selectivity for these films [20–25]. The LC monomer **C6-CH<sub>3</sub>** is commercially available and often used in LC polymer films. The LC monomer **C6-Cl** was synthesised and characterised following a literature procedure [15], while **C6-CN** and **C6-C<sub>6</sub>H<sub>5</sub>** were synthesised according to Scheme 1. The synthetic preparations are described in the supporting information. Characterisation by  $^1\text{H}$  and  $^{13}\text{C}$  nuclear magnetic resonance (NMR) and mass spectroscopy (MALDI-TOF MS) confirmed the successful formation of all synthesised molecules.

The LC behaviour of the molecules was studied by determining the phase transition temperatures with differential scanning calorimetry (DSC) and polarising optical microscopy (POM). The results are shown in Table 2 (Figure S1-S5 for DSC and POM).

All LC monomers exhibit a nematic phase but at different temperature ranges. The compounds **C6-CN**, **C6-Cl** and **C6-CH<sub>3</sub>** have similar isotropic-nematic phase transitions but **C6-C<sub>6</sub>H<sub>5</sub>**, which has the largest substituent of all LCs used in this study, has the lowest isotropic-nematic phase transition [26,27]. Because the viscosity of the pure **C6-C<sub>6</sub>H<sub>5</sub>** monomer was too high to prepare aligned films, LC mixtures consisting of **C6-C<sub>6</sub>H<sub>5</sub>** with **C6-CH<sub>3</sub>** were prepared and characterised with

**Table 1.** The kinetic diameter, critical temperature and quadrupole moment of the measured gasses (He,  $\text{CO}_2$ ,  $\text{CH}_4$  and Xe) [19].

Gas species	Kinetic diameter [Å]	Critical temperature [K]	Quadrupole moment [ $\text{cm}^2$ ] · $10^{40}$
He	2.60	5.19	0.00
$\text{CO}_2$	3.30	304.13	−13.71
$\text{CH}_4$	3.80	190.55	0.00
Xe	3.96	289.77	0.00

**Table 2.** Phase transitions and fabrication conditions of all LCs used in this study.

Compound/Mixture	Isotropic [ $^\circ\text{C}$ ]	Nematic [ $^\circ\text{C}$ ]	Polymerisation temperature [ $^\circ\text{C}$ ]	Cooling rate [ $^\circ\text{C}/\text{min}$ ]
<b>C6-CN</b>	>104	104-96	100	2
<b>C6-Cl</b>	>110	110-99	100	2
<b>C6-CH<sub>3</sub></b>	>113	113-86	100	2
<b>C6-C<sub>6</sub>H<sub>5</sub></b>	>30	30-20	-	-
<b>C6-C<sub>6</sub>H<sub>5</sub> with 20 wt% C6-CH<sub>3</sub></b>	>39	39-30	32	1

DSC and POM. Compositions of **C6-C<sub>6</sub>H<sub>5</sub>** with 20 wt% **C6-CH<sub>3</sub>** and more could be used to fabricate aligned films, hence an LC mixture consisting of **C6-C<sub>6</sub>H<sub>5</sub>** with 20 wt% **C6-CH<sub>3</sub>** was used.

### 3.2. Preparation and characterisation of liquid crystalline films

Planar aligned nematic LC films were prepared by mixing the LCs with a photoinitiator and inhibitor and subsequently incorporating the LC mixtures in glass cells with alignment layers. After heat treatment, the LC mixtures were photopolymerised to fixate the aligned nematic morphology. Subsequent opening of the glass cells in hot water yielded free-standing nematic LC films. FT-IR spectra of the LC films showed full conversion of the acrylate moieties after photopolymerisation (Figure S6).

POM shows the planar alignment of all films with dark images under parallel conditions and bright images under 45° tilt (Figure S7). Wide-angle X-ray scattering (WAXS) and medium-angle X-ray scattering (MAXS) were measured to further confirm the morphology and alignment of the prepared films (Figure 2).

The two-dimensional (2D) WAXS spectra in Figure 2 show for all films' diffraction spots, indicating aligned LCs. The **C6-CH<sub>3</sub>** and **C6-C<sub>6</sub>H<sub>5</sub>** films show only diffraction spots in the wide-angle region (Figure 2(c,d)), which is characteristic for a nematic molecular organisation. Additionally, the **C6-CN** and **C6-Cl** films show weak diffused diffraction spots in the medium-angle region (Figure 2(e,f)), which is characteristic for a nematic cybotactic morphology having localised nanometre-sized smectic domains [28,29]. The intermolecular spacing, which corresponds to the

intermolecular stacking of the molecules, is not affected by the different substituents and was found to be similar for all films, varying between 4.6 and 4.7 Å. The above results show the successful fabrication of the planar aligned nematic LC films.

### 3.3. Single gas permeation and selectivity of nematic LC films

The effect of various substituents on the gas permeation data and ideal gas selectivities of He/CH<sub>4</sub>, CO<sub>2</sub>/CH<sub>4</sub> and He/CO<sub>2</sub> are presented in Figure 3 (see Table S2 and S3 for all permeation and ideal selectivity values).

Figure 3(a) shows that the permeability of all gasses is affected by the substituents on the LC monomers, showing the lowest permeabilities for the **C6-CN** films and the highest permeabilities for the **C6-C<sub>6</sub>H<sub>5</sub>** films (**C6-CN** < **C6-Cl** < **C6-CH<sub>3</sub>** < **C6-C<sub>6</sub>H<sub>5</sub>**). This most likely originates from the different steric sizes of the substituents on the central aromatic cores of the LC monomers that affects the packing density of the polymer chains. A frequently used system for evaluation of the relative steric size of functional groups is the Winstein-Holness A-value system [30–33], which states that the relative steric size of the substituents used in this study is **CN** < **Cl** < **CH<sub>3</sub>** < **C<sub>6</sub>H<sub>5</sub>**. Comparing the relative steric sizes of the substituents with the measured gas permeabilities of the **C6-CN**, **C6-Cl**, **C6-CH<sub>3</sub>** and **C6-C<sub>6</sub>H<sub>5</sub>** films reveal a relationship between the increasing steric size of the substituents and increasing gas permeabilities. Here, a larger steric size of the substituent leads to a larger overall free volume and/or size of the free volume elements in the film, resulting in higher diffusion rates through the films and therefore higher gas permeabilities for films with larger substituents. However, next to

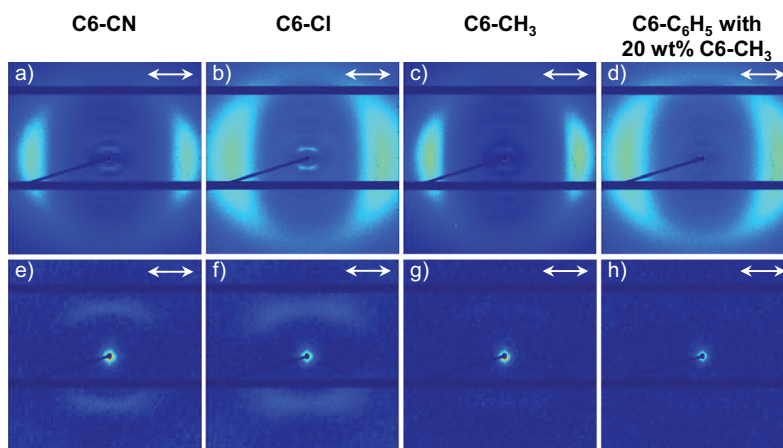


**Figure 2.** (Color online) WAXS (top row) and MAXS (bottom row) spectra of the prepared nematic LC films with different substituents. (a, e) **C6-CN**, (b, f) **C6-Cl**, (c, g) **C6-CH<sub>3</sub>**, (d, h) **C6-C<sub>6</sub>H<sub>5</sub>** with 20 wt% **C6-CH<sub>3</sub>**. The single arrow shows the alignment direction.

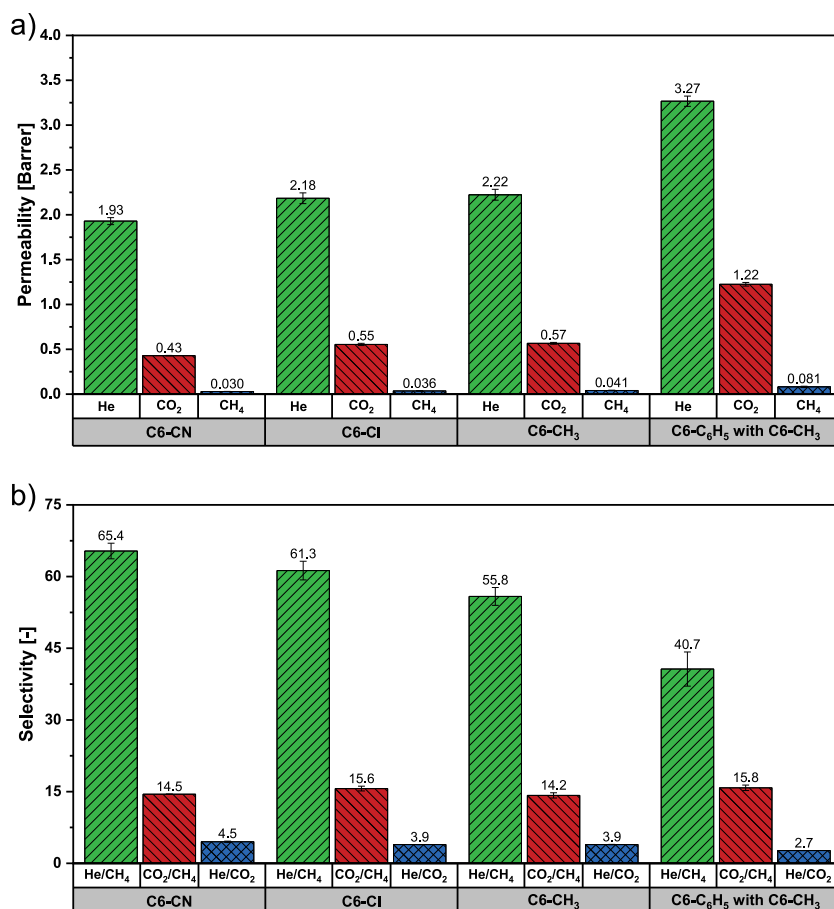


**Figure 3.** (Color online) Gas permeation data and ideal gas selectivities of nematic LC films with cyano, chloro, methyl and phenyl substituents. (a) single gas permeability (He, CO<sub>2</sub> and CH<sub>4</sub>) of **C6-CN**, **C6-Cl**, **C6-CH<sub>3</sub>** and **C6-C<sub>6</sub>H<sub>5</sub>** with 20 wt% **C6-CH<sub>3</sub>** films measured at 40°C and 6 bar feed pressure. (b) Ideal gas selectivities (He/CH<sub>4</sub>, CO<sub>2</sub>/CH<sub>4</sub> and He/CO<sub>2</sub>) of **C6-CN**, **C6-Cl**, **C6-CH<sub>3</sub>** and **C6-C<sub>6</sub>H<sub>5</sub>** with 20 wt% **C6-CH<sub>3</sub>** films at 40°C. The small error bars represent the spread of two independently prepared membranes, where each membrane is measured in triplicate.

the steric size of the substituents also the small difference in molecular organisation between the films might affect the gas permeabilities [14,34].

Contrary to the gas permeability, the ideal gas selectivity of He/CH<sub>4</sub> and He/CO<sub>2</sub> decreases with increasing steric size of the substituents (Figure 3(b)). This results in the highest selectivities for the **C6-CN** films (respectively 65.4 for He/CH<sub>4</sub> and 4.5 for He/CO<sub>2</sub>) and the lowest selectivities for the **C6-C<sub>6</sub>H<sub>5</sub>** films (respectively 40.7 for He/CH<sub>4</sub> and 2.7 for He/CO<sub>2</sub>). This decrease in selectivity towards He can be attributed to the increase of the total free volume and/or size of the free volume elements with increasing steric size of the substituents. This effect also affects the diffusion of CO<sub>2</sub> and CH<sub>4</sub>, which have larger kinetic diameters than He, resulting in lower selectivities towards He. Counterintuitively, the CO<sub>2</sub>/CH<sub>4</sub> selectivity is similar for all films. Although one would expect that the CO<sub>2</sub>/CH<sub>4</sub> selectivity decreases with increasing steric size of the substituents (C6-CN > C6-Cl > C6-CH<sub>3</sub> > C6-C<sub>6</sub>H<sub>5</sub>), the difference in kinetic diameter between CO<sub>2</sub> and CH<sub>4</sub>

(respectively 3.30 Å and 3.80 Å) is smaller compared to the difference between the kinetic diameter of He and CH<sub>4</sub> (respectively 2.60 Å and 3.80 Å), resulting in more comparable diffusion rates of CO<sub>2</sub> and CH<sub>4</sub> through the film. This diminishes the effect of steric size of the substituents and leads to very similar CO<sub>2</sub>/CH<sub>4</sub> selectivities for all films. Secondly, the relatively low cyano and chloro content in the **C6-CN** and **C6-Cl** films does not give significant improvement in CO<sub>2</sub> permeability and selectivity compared to the **C6-CH<sub>3</sub>** and **C6-C<sub>6</sub>H<sub>5</sub>** films and therefore results in comparable CO<sub>2</sub>/CH<sub>4</sub> selectivities for all films.

### 3.4. Gas sorption and diffusion of nematic LC films

The effect of the different substituents on the gas separation properties of nematic LC films was further studied to identify the underlying mechanism for the observed differences. CO<sub>2</sub> sorption in the films was measured to determine the solubility coefficient and subsequently extract the diffusion coefficient using Equation (2).



**Table 3.** CO<sub>2</sub> permeabilities, CO<sub>2</sub> solubility coefficients measured at 6 bar and 40°C and the associated calculated diffusion coefficients of all films.

Film	P	S	D
	$\left[\frac{\text{cm}^3(\text{STP}) \cdot \text{cm}}{\text{cm}^2 \cdot \text{s} \cdot \text{cmHg}}\right] \cdot 10^{-10}$	$\left[\frac{\text{cm}^3(\text{STP})}{\text{cm}^3 \cdot \text{cmHg}}\right] \cdot 10^{-3}$	$\left[\frac{\text{cm}^2}{\text{s}}\right] \cdot 10^{-9}$
C6-CN	0.43	8.05	5.33
C6-Cl	0.55	8.83	6.28
C6-CH <sub>3</sub>	0.57	8.38	6.76
C6-C <sub>6</sub> H <sub>5</sub> with 20 wt% C6-CH <sub>3</sub>	1.22	7.37	16.63

Unfortunately, only CO<sub>2</sub> sorption could be measured because He was used for the buoyancy measurements and the CH<sub>4</sub> sorption was for all films too low to obtain accurate values. The CO<sub>2</sub> permeabilities, CO<sub>2</sub> solubility coefficients and associated diffusion coefficients of all films are shown in Table 3.

Table 3 shows that the solubility coefficient of CO<sub>2</sub> is similar for all films, meaning that the increase in CO<sub>2</sub> permeability with increasing steric size of the substituents can be completely attributed to an increase in the diffusion coefficient. All films exhibit similar CO<sub>2</sub> solubility coefficients, elucidating that the polar cyano and chloro groups in the C6-CN and C6-Cl films do not lead to improved CO<sub>2</sub>-polymer matrix interactions. This explains the similar CO<sub>2</sub>/CH<sub>4</sub> selectivities (as depicted in Figure 3). Consequently, the polarity of the cyano and chloro groups in the C6-CN and C6-Cl films does not affect the gas separation performance of these films and the difference in performances solely depends on steric effects of the substituents. Contrary to the solubility coefficient, the diffusion coefficient increases with increasing steric size of the substituents, resulting in a 3 times higher diffusion coefficient for the C6-C<sub>6</sub>H<sub>5</sub> films compared to the C6-CN films. The similar solubility coefficients of the films indicate that not the total free volume [35], but the size of the free volume elements in the films increase with increasing size of the substituents. This finding is in accordance with the intermolecular spacing of the molecules (section 3.2), which is similar for all films, indicating that the overall

free volume in the films is similar regardless of the size of the substituents. However, although the intermolecular spacing is similar for all films, the size of the free volume pockets in the films likely increase with increasing size of the substituents. These increased free volume pockets increase the diffusion coefficients of all gasses and result in higher permeabilities for the films containing larger substituents. The diffusion coefficient of the larger CO<sub>2</sub> and CH<sub>4</sub> gasses is more affected by the size of the free volume elements compared to the smaller He, resulting in lower selectivities towards He with increasing steric size of the substituents [36,37].

### 3.5. The effect of kinetic diameter of different gas species on the gas separation properties

The effect of the kinetic diameter on the gas separation properties of the LC films was studied in more detail by comparing single gas permeation and sorption data of CO<sub>2</sub> and Xe because both have similar critical temperatures but Xe has a larger kinetic diameter. Due to the scarcity of Xe, its permeation and sorption were only measured for the C6-CH<sub>3</sub> and C6-C<sub>6</sub>H<sub>5</sub> films. For comparison, the permeation data of He and CH<sub>4</sub> are also plotted in Figure 4.

Figure 4(a) shows that irrespective of the LC substituent He has the highest permeability followed by CO<sub>2</sub>, CH<sub>4</sub> and Xe following the order of kinetic diameter and critical temperature. As discussed in section 3.3, the larger steric size of the phenyl substituent in the C6-C<sub>6</sub>

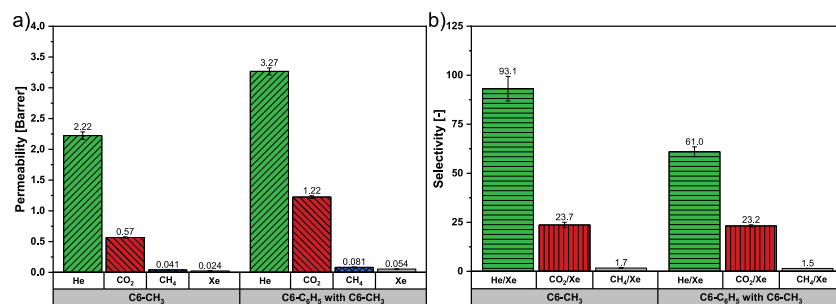


**Figure 4.** (Color online) Gas permeation data and ideal gas selectivities of nematic LC films with methyl and phenyl substituents. (a) single gas permeability (He, CO<sub>2</sub>, CH<sub>4</sub> and Xe) of C6-CH<sub>3</sub> and C6-C<sub>6</sub>H<sub>5</sub> with 20 wt% C6-CH<sub>3</sub> films measured at 40°C and 6 bar feed pressure. (b) Ideal gas selectivities (He/Xe, CO<sub>2</sub>/Xe and CH<sub>4</sub>/Xe) of C6-CH<sub>3</sub> and C6-C<sub>6</sub>H<sub>5</sub> with 20 wt% C6-CH<sub>3</sub> films at 40°C. The small error bars represent the spread of two independently prepared membranes, where each membrane is measured in triplicate.

**Table 4.** CO<sub>2</sub> and Xe permeabilities and solubility coefficients measured at 40°C and 6 bar and the associated calculated diffusion coefficients of the C6-CH<sub>3</sub> and C6-C<sub>6</sub>H<sub>5</sub> films.

Film	Gas species	P	S	D
		$\left[\frac{\text{cm}^3(\text{STP})\text{m}}{\text{cm}^2\text{scmHg}}\right] \cdot 10^{-10}$	$\left[\frac{\text{cm}^3(\text{STP})}{\text{cm}^3\text{.cmHg}}\right] \cdot 10^{-3}$	$\left[\frac{\text{cm}^2}{\text{s}}\right] \cdot 10^{-9}$
C6-CH <sub>3</sub>	CO <sub>2</sub>	0.57	8.38	6.76
	Xe	0.02	6.89	0.349
C6-C <sub>6</sub> H <sub>5</sub> with 20 wt% C6-CH <sub>3</sub>	CO <sub>2</sub>	1.22	7.37	16.63
	Xe	0.05	6.38	0.847

H<sub>5</sub> films result in larger free volume pockets in the films and therefore higher permeabilities for all gasses (including Xe) but lower ideal gas selectivities towards He when compared to the C6-CH<sub>3</sub> films with the smaller sized methyl substituent. Figure 4(b) shows that the selectivity towards Xe for both the C6-CH<sub>3</sub> and C6-C<sub>6</sub>H<sub>5</sub> films decreases for gas pairs with more similar kinetic diameters, resulting in the highest selectivity for He/Xe > CO<sub>2</sub>/Xe > CH<sub>4</sub>/Xe. The CO<sub>2</sub> and Xe permeabilities, solubility coefficients and the associated calculated diffusion coefficients for the C6-CH<sub>3</sub> and C6-C<sub>6</sub>H<sub>5</sub> with 20 wt% C6-CH<sub>3</sub> films are shown in Table 4.

Table 4 shows that the slightly lower critical temperature of Xe compared to CO<sub>2</sub> (289.77 versus 304.13 K) leads to a 1.2 times lower solubility coefficient for Xe compared to that of CO<sub>2</sub> for both films. However, due to its larger size, the diffusion coefficient of Xe is approximately 20 times lower than the diffusion coefficient of CO<sub>2</sub>, which means that the low Xe permeability mainly originates from the low diffusion rate of Xe through the film.

## Conclusions

New LC 1,4-phenylene bis(4-((6-(acryloyloxy)hexyl)oxy)benzoate)s derivatives were successfully synthesised and fully characterised. The gas permeation performance for He, CO<sub>2</sub>, CH<sub>4</sub> and Xe of well-aligned free-standing planar aligned nematic LC polymer films with respective cyano, chloro, methyl and phenyl substituents was investigated.

Single gas permeation of He, CO<sub>2</sub> and CH<sub>4</sub> and gas sorption of CO<sub>2</sub> demonstrated that the gas permeability of the nematic LC films increases with increasing steric size of the substituents, while the ideal gas selectivities towards He decrease with increasing steric size of the substituents. An increasing diffusion coefficient with increasing substituent steric size was responsible for these effects and not the solubility of the gases in the polymer matrix. The effect of kinetic diameter is most obvious from a 20-fold reduction of the diffusion coefficient of the larger Xe compared to the smaller CO<sub>2</sub>, resulting in considerably lower Xe permeabilities.

## Acknowledgment

This research was part of the research programme START-UP with project number 740.018.005, which is financed by the Dutch Organization for Scientific Research (NWO). The authors want to thank Anna Casimiro of the Eindhoven University of Technology for her help with the MAXS/WAXS measurements, Lou Xianwen of the Eindhoven University of Technology for his help with MALDI-TOF measurements and Juan Carlos de Galan (Zaragoza University) and Jannet van der Veen (Philips Research) for their assistance with the synthesis of C6-CN and C6-C<sub>6</sub>H<sub>5</sub>.


## Disclosure statement

No potential conflict of interest was reported by the author(s).

## Funding

The work was supported by the Dutch Organization for Scientific Research (NWO) [START-UP, project number 740.018.005].

## ORCID

Joey Kloos  <http://orcid.org/0000-0002-7821-7256>  
 Johan Lub  <http://orcid.org/0000-0002-3812-1735>  
 Kitty Nijmeijer  <http://orcid.org/0000-0002-1431-2174>  
 Albert P. H. J. Schenning  <http://orcid.org/0000-0002-3485-1984>

## CRedit authorship contribution statement

**Joey Kloos:** Conceptualization, Methodology, Validation, Formal analysis, Investigation, Writing – Original Draft, Writing – Review & Editing, Visualization. **Johan Lub:** Formal analysis, Investigation, Writing – Review & Editing. **Menno Houben:** Formal analysis, Investigation, Writing – Review & Editing. **Zandrie Borneman:** Conceptualization, Supervision, Writing – Review & Editing. **Kitty Nijmeijer:** Conceptualization, Supervision, Writing – Review & Editing, Project administration, Funding acquisition. **Albert Schenning:** Conceptualization, Writing – Review & Editing.

## References

- [1] Dierking I. Textures of liquid crystals. Weinheim: Wiley-Vch Verlag GmbH; 2003.

- [2] Kloos J, Joosten N, Schenning A, et al. Self-assembling liquid crystals as building blocks to design nanoporous membranes suitable for molecular separations. *J Membr Sci.* 2021;620:118849.
- [3] Luggar J, Mulder DJ, Sijbesma R, et al. Nanoporous polymers based on liquid crystals. *Materials (Basel).* 2018;11:104.
- [4] Andrienko D. Introduction to liquid crystals. *J Mol Liq.* 2018;267:520–541.
- [5] Taylor GW. Introduction to liquid crystals. *Ferroelectrics.* 1987;73:265.
- [6] Basu S, Khan AL, Cano-Odena A, et al. Membrane-based technologies for biogas separations. *Chem Soc Rev.* 2010;39:750–768.
- [7] Bernardo P, Drioli E, Golemme G. Membrane gas separation: a review/state of the art. *Ind Eng Chem Res.* 2009;48:4638–4663.
- [8] Sanders DF, Smith ZP, Guo R, et al. Energy-efficient polymeric gas separation membranes for a sustainable future: a review. *Polymer (Guildf).* 2013;54:4729–4761.
- [9] Rufford TE, Smart S, Watson GCY, et al. The removal of CO<sub>2</sub> and N<sub>2</sub> from natural gas: a review of conventional and emerging process technologies. *J Pet Sci Eng.* 2012;94–95:123–154.
- [10] Kim S, Lee YM. High performance polymer membranes for CO<sub>2</sub> separation. *Curr Opin Chem Eng.* 2013;2:238–244.
- [11] Wang S, Li X, Wu H, et al. Advances in high permeability polymer-based membrane materials for CO<sub>2</sub> separations. *Energy Environ Sci.* 2016;9:1863–1890.
- [12] Hamid MRA, Jeong HK. Recent advances on mixed-matrix membranes for gas separation: opportunities and engineering challenges. *Korean J Chem Eng.* 2018;35:1577–1600.
- [13] Sridhar S, Smitha B, Aminabhavi TM. Separation of carbon dioxide from natural gas mixtures through polymeric membranes - a review. *Sep Purif Rev.* 2007;36:113–174.
- [14] Kloos J, Jansen N, Houben M, et al. On the order and orientation in liquid crystalline polymer membranes for gas separation. *Chem Mater.* 2021;33:8323–8333.
- [15] Kloos J, Houben M, Lub J, et al. Tuning the gas separation performances of smectic liquid crystalline polymer membranes by molecular engineering. *Membranes (Basel).* 2022;805:805.
- [16] Bergeron RJ, Wiegand J, McManis JS, et al. The design, synthesis, and evaluation of organ-specific iron chelators. *J Med Chem.* 2006;49:7032–7043.
- [17] Koros WJ, Fleming GK, Jordan SM, et al. Polymeric membrane materials for solution-diffusion based permeation separations. *Prog Polym Sci.* 1988;13:339–401.
- [18] Wijmans JG, Baker RW. The solution-diffusion model: a review. *J Membr Sci.* 1995;107:1–21.
- [19] Rallapalli P, Prasanth KP, Patil D, et al. Sorption studies of CO<sub>2</sub>, CH<sub>4</sub>, N<sub>2</sub>, CO, O<sub>2</sub> and Ar on nanoporous aluminum terephthalate [MIL-53(Al)]. *J Porous Mater.* 2011;18:205–210.
- [20] Ghosal K, Freeman BD. Gas separation using polymer membranes: an overview. *Polym Adv Technol.* 1994;5:673–697.
- [21] Wang X, Wilson TJ, Maroon CR, et al. Vinyl-addition fluoroalkoxysilyl-substituted polynorbornene membranes for CO<sub>2</sub>/CH<sub>4</sub> separation. *ACS Appl Polym Mater.* 2022. DOI:10.1021/acsp.1c01833.
- [22] Hellums MW, Koros WJ, Husk GR, et al. Fluorinated polycarbonates for gas separation applications. *J Membr Sci.* 1989;46:93–112.
- [23] Kadir Khan F, Goh PS, Ismail AF, et al. Recent advances of polymeric membranes in tackling plasticization and aging for practical industrial CO<sub>2</sub>/CH<sub>4</sub> applications—a review. *Membranes (Basel).* 2022;12:71.
- [24] Mahurin SM, Yeary JS, Baker SN, et al. Ring-opened heterocycles: promising ionic liquids for gas separation and capture. *J Membr Sci.* 2012;401–402:61–67.
- [25] Bara JE, Gabriel CJ, Hatakeyama ES, et al. Improving CO<sub>2</sub> selectivity in polymerized room-temperature ionic liquid gas separation membranes through incorporation of polar substituents. *J Membr Sci.* 2008;321:3–7.
- [26] Averyanov EM. Steric effects of substituents in mesogens and phase transition temperatures in uniaxial liquid crystals. *Liq Cryst.* 1987;2:491–504.
- [27] Osman MA. Molecular structure and mesomorphic properties of thermotropic liquid crystals. II. Terminal Substituents. *Z Naturforsch.* 1983;38:693–697.
- [28] McMillan WL. X-ray scattering from liquid crystals. I. cholesteryl nonanoate and myristate. *Phys Rev A.* 1972;6:936–947.
- [29] Nasrin L, Nasir AK, Yoshizawa A, et al. Nematic - Cybotactic nematic phase transition in a liquid crystal: a dielectric spectroscopic study. *Mater Res Express.* 2019;6:115105.
- [30] Winstein S, Holness NJ. Neighboring carbon and hydrogen. XIX. t-butylcyclohexyl derivatives. quantitative conformational analysis. *J Am Chem Soc.* 1955;77:5562–5578.
- [31] Anslyn EV, Dougherty DA. *Modern Physical Organic Chemistry.* Sausalito: University Science Books; 2005.
- [32] Förster H, Vögtle F. Steric interactions in organic chemistry: spatial requirements of substituents. *Angew Chemie Int Ed English.* 1977;16:429–441.
- [33] Solel E, Ruth M, Schreiner PR. London dispersion helps refine steric  $\sigma$ -values: dispersion energy donor scales. *J Am Chem Soc.* 2021;143:20837–20848.
- [34] Bara JE, Kaminski AK, Noble RD, et al. Influence of nanostructure on light gas separations in cross-linked lyotropic liquid crystal membranes. *J Membr Sci.* 2007;288:13–19.
- [35] Hu CC, Chang CS, Ruaan RC, et al. Effect of free volume and sorption on membrane gas transport. *J Membr Sci.* 2003;226:51–61.
- [36] Haraya K, Hwang ST. Permeation of oxygen, argon and nitrogen through polymer membranes. *J Membr Sci.* 1992;71:13–27.
- [37] Thornton AW, Nairn KM, Hill AJ, et al. New relation between diffusion and free volume: I. Predicting gas diffusion. *J Membr Sci.* 2009;338:29–37.